JACS
JOURNAL OF THE AMERICAN CHEMICAL SOCIETY
Article
pubs.acs.org/JACS

Unusual Reaction of [NiFe]-Hydrogenases with Cyanide

Suzannah V. Hexter, Min-Wen Chung, Kylie A. Vincent,* and Fraser A. Armstrong*

Inorganic Chemistry Laboratory, Department of Chemistry, University of Oxford, South Parks Road, Oxford OX1 3QR, United Kingdom

Supporting Information

ABSTRACT: Cyanide reacts rapidly with [NiFe]-hydrogenases (hydrogenase-1 and hydrogenase-2 from *Escherichia coli*) under mild oxidizing conditions, inhibiting the electrocatalytic oxidation of hydrogen as recorded by protein film electrochemistry. Electrochemical, EPR, and FTIR measurements show that the final enzyme product, formed within a second (even under 100% H_2), is the resting state known as Ni−B, which contains a hydroxido-bridged species, $Ni^{III}-\mu(OH)-Fe^{II}$, at the active site. "Cyanide inhibition" is easily reversed because it is simply the reductive activation of Ni−B. This paper brings back into focus an observation originally made in the 1940s that cyanide inhibits microbial H_2 oxidation and addresses the interesting mechanism by which cyanide promotes the formation of Ni−B. As a much stronger nucleophile than hydroxide, cyanide binds more rapidly and promotes oxidation of Ni^{II} to Ni^{III}; however, it is quickly replaced by hydroxide which is a far superior bridging ligand.

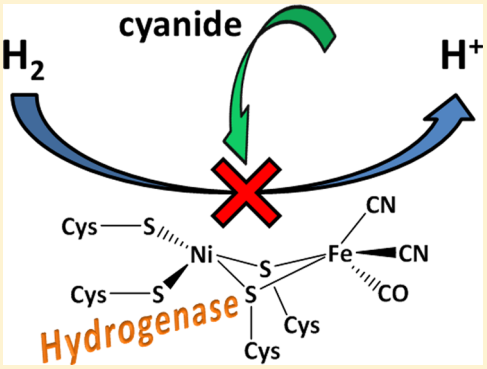

INTRODUCTION

Hydrogenases are abundant enzymes which catalyze the production and oxidation of molecular H_2 in microbes. The two main classes, [NiFe]- and [FeFe]-hydrogenases, are named according to the metal ions present in their bimetallic active site, which in both classes contain biologically unusual CO and CN^- endogenous ligands. Many [NiFe]-[1−4] and [FeFe]-hydrogenases[5] react rapidly with exogenous CO, resulting in a decrease in catalytic activity as the incoming CO competes with H_2. Activity is restored upon removal of CO from the solution.[1] Surprisingly, however, little is known about the effect of exogenous cyanide on these enzymes. As early as 1942, Lee et al.[6] reported the inhibitory effect of cyanide on the H_2 oxidation activity of whole cell samples of *Azotobacter vinelandii*. In 1952, Hyndman et al.[7] observed similar results with cell-free extracts of *A. vinelandii* hydrogenase. Seefeldt and Arp[8] published the first study on the affect of cyanide on purified *A. vinelandii* hydrogenase in 1989. Using spectrophotometric assay methods, they found cyanide to inhibit the enzyme irreversibly under oxidizing conditions. Addition of a reductant during the course of the cyanide-dependent inhibition immediately halted the inactivation process but did not result in the reactivation of the enzyme which had previously been inactivated.

Crystal structures of [NiFe]-hydrogenases reveal two endogenous CN^- and one CO ligand bound to the Fe(II) ion at the active site, as shown in Figure 1.[9,10] The Fe(II) ion, which is redox-inactive throughout catalysis,[11] is also bound to two cysteine residues which form bridges to the Ni atom. The Ni ion, which probably cycles between Ni(I), Ni(II), and Ni(III) throughout catalysis, is also coordinated by two further cysteine thiolates. The four cysteines together retain the active site in place within the large subunit of the heterodimeric enzyme. The small subunit contains three Fe−S clusters which act as a relay, shuttling electrons between the buried active site and the surface of the protein. A network of hydrophobic gas channels which appear to end at the Ni atom[12,13] allows small molecules to reach the active site.

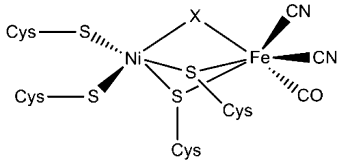

Figure 1. Structure of the active site of [NiFe]-hydrogenases. The ligand labeled X is established to be OH^- in Ni−B.

Exogenous carbon monoxide, mentioned above as a competitive inhibitor, appears to bind as a terminal ligand to the Ni.[14] In contrast, many studies have investigated the nature of additional ligands "X" that bind in the bridging position between Fe and Ni atoms. A state known as Ni−C, formed under H_2 and long proposed to be a catalytic intermediate (Scheme 1), contains a hydrido ligand that is coordinated to Ni(III) and oriented in the bridging position.[15,16] The bridging position is also occupied in oxidized inactive states of the enzyme, the most established by far being Ni−B, which is formed at high potentials, both anaerobically and in the presence of O_2. Also termed "Ready" because it is reactivated very rapidly upon reduction, Ni−B contains a OH^- ligand in the bridging position.[17,18] Exclusive formation of the Ni−B

Received: May 17, 2014
Published: July 8, 2014

dx.doi.org/10.1021/ja504942h | J. Am. Chem. Soc. 2014, 136, 10470−10477

Scheme 1. Spectroscopically Well-Established Active and Inactive States of [NiFe]-Hydrogenases under Anaerobic Conditions[a]

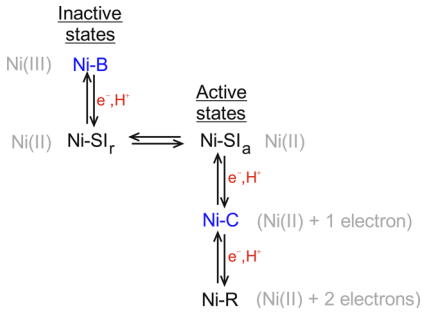

[a]States detectable by EPR are shown in blue. The changing oxidation states (formal electron counts starting from Ni^{II}) are shown in gray. Adapted from ref 24. Copyright 2007 American Chemical Society.

"resting" state in the presence of O_2 (avoiding trapped, partly reduced oxygen species) is important in a special class of hydrogenases known as "O_2-tolerant" [NiFe]-hydrogenases, which can function indefinitely in the presence of O_2.[19,20] A sulfido or hydrosulfido ligand can also occupy the bridging position in an oxidized inactive state analogous to Ni–B.[21,22] The relationship between the Ni–B state and the active states of the enzyme is summarized in Scheme 1.

How does cyanide react ? Important new insight into the reaction taking place with exogenous cyanide is now provided by protein film electrochemistry (PFE) in which the enzyme is directly adsorbed onto an electrode (typically a pyrolytic graphite "edge" (PGE) electrode) creating an electroactive film.[23,24] Provided that interfacial (electrode–enzyme) electron transfer is fast, the catalytic activity of the enzyme, which is directly proportional to the catalytic current, is recorded as a direct and continuous function of the electrode potential. It is thus possible to induce and observe reactions that alter the activity of an enzyme and to measure their rates and the characteristic potentials needed for them to occur. A detailed and quantitative description of enzyme activity is thus obtained that complements information provided by other methods. Using PFE in conjunction with electron paramagnetic resonance (EPR) spectroscopy and attenuated total reflectance infrared (ATR-IR) spectroelectrochemistry, we now demonstrate and account for a rapid and transient reaction that occurs when cyanide is added to [NiFe]-hydrogenases.

MATERIALS AND METHODS

Materials. Samples of hydrogenase-1 and hydrogenase-2 from *Escherichia coli* (abbreviated Hyd1 and Hyd2, respectively) were prepared as described previously.[25] All reagents were of at least analytical grade. Throughout, HEPES buffer refers to 4-[2-hydroxyethyl]-1-piperazine-*N*-2-ethanesulfonic acid (Fisher).

Protein Film Electrochemistry. Protein Film Electrochemistry experiments were performed in an anaerobic glovebox (Belle Technologies or M Braun) containing a N_2 atmosphere (O_2 < 3 ppm). Measurements were made using an electrochemical analyzer (Autolab PGSTAT30) controlled by Nova software (EcoChemie). A pyrolytic graphite "edge" rotating disk electrode (geometric surface area 0.03 cm^2) was used as the working electrode in conjunction with an electrode rotator (EcoChemie) which fitted snugly into the working compartment of the sealed electrochemical glass cell. The three-electrode configuration also featured a Pt wire counter electrode and a saturated calomel reference electrode (SCE) housed in a side arm (maintained at 25 °C) containing 0.10 M NaCl and connected to the working compartment via a Luggin capillary. Potentials are quoted with respect to the standard hydrogen electrode (SHE) using the correction $E_{SHE} = E_{SCE} + 242$ mV at 25 °C. All solutions were prepared using purified water (Millipore, 18 MΩ·cm) and a mixed buffer system[26] titrated to the desired pH at the experimental temperature. Gas inlets into the working compartment of the cell allowed experiments to be performed under gas mixtures of H_2 (premier grade, Air Products) and N_2 (BOC gases), controlled using precision mass flow controllers (Sierra Instruments). To prepare each enzyme film, the PGE electrode surface was abraded with P400 Tufbak Durite sandpaper before being placed in a sonicator for approximately 5 s and then rinsed with purified water. Enzyme solution (1 μL of approximately 20 μM) was then pipetted onto the electrode surface and left for approximately 15 s to adsorb strongly before excess enzyme was removed by pipet. The adsorbed enzyme was activated under H_2 by poising the potential at −560 mV for 300 s between cyclic voltammetry scans (cycling between −560 and 240 mV) until the maximum current reached in successive scans had stabilized, indicating that activation was complete. Data analysis was performed using OriginPro 8 and Excel Solver software.

Electron Paramagnetic Resonance Spectroscopy. Continuous-wave EPR experiments were performed using an X-band Bruker EMX spectrometer (Bruker BioSpin GmbH, Germany) with an X-band super-high-sensitivity probehead (Bruker) equipped with a low-temperature helium flow cryostat (Oxford Instruments CF935). Data analysis was performed using the program EasySpin.[27] Sample preparation was carried out within an anaerobic glovebox (O_2 < 3 ppm) as follows.

Preparation of Equilibrated Samples at a Defined Potential. Hydrogenase-2 samples in 0.1 M HEPES, 0.1 M NaCl, 10% glycerol at pH 7, 25 °C, were transferred to a redox titration cell similar to that first described by Dutton.[28] The equilibrium solution potential was determined using a two-electrode system: the working electrode was the platinum ring of a combination electrode (Mettler Toledo, InLab Redox Micro), and the reference electrode was a micro-Ag/AgCl electrode (WPI, DRIREF-2). Potentials are quoted with respect to SHE using the correction $E_{SHE} = E_{Ag/AgCl} + 195$ mV at 20 °C. The cell featured a water jacket to achieve thermostatic control, and a stirrer bar ensured constant mixing of the enzyme solution. Samples were first activated under 100% H_2 at 20 °C until equilibration to the $2H^+/H_2$ potential was reached after about 1 h, at which point the H_2 was flushed from the cell with pure Ar (Pureshield, BOC gases). Aliquots of a solution of $K_3[Fe(CN)_6]$ were then added to the solution until the desired potential was reached. The cell was kept under a positive gas pressure which allowed enzyme solution to be transferred from the cell into an EPR tube via a stainless steel tube. The sample was then flash frozen using a coldfinger attachment containing liquid-nitrogen-cooled ethanol within the glovebox.

Preparation of Samples at Short Times Using a Freeze-Quench Method. Samples were prepared by using the sample handling unit from a stopped-flow instrument (Hi-Tech) adapted in-house to allow reagents to be rapidly mixed (under pneumatic pressure) at room temperature and sprayed into a funnel containing isopentane cooled to liquid nitrogen temperature. The funnel was attached to an EPR tube, into which the frozen product was transferred. Prior to mixing, the solution in each syringe was as follows: (i) Hyd2 (approximately 50 μM) in 0.10 M HEPES buffer, pH 7, containing 10% glycerol and 0.10 M NaCl, which had been activated under a flow of H_2 following which the H_2 was flushed out with Ar as described above; (ii) either $K_3[Fe(CN)_6]$ only or $K_3[Fe(CN)_6]$ and KCN dissolved in 0.10 M HEPES buffer, pH 7, containing 10% glycerol and 0.10 M NaCl, leading to a final concentration of 4.8 mM $[Fe(CN)_6]^{3-}$ and, if used, 5.1 mM cyanide in the sample.

Attenuated Total Reflectance Infrared Spectroelectrochemistry. Infrared spectroelectrochemistry experiments were performed in an anaerobic glovebox (<1 ppm of O_2) at a working electrode comprising Hyd2 trapped in a mixture of the ion-exchange resin Nafion 117 and carbon black particles on a silicon multibounce ATR prism, as described previously.[29] A miniature SCE reference electrode, constructed in-house, and a Pt wire counter

dx.doi.org/10.1021/ja504942h | J. Am. Chem. Soc. 2014, 136, 10470–10477

electrode were inserted into the solution compartment of the cell. A pH 7 Nafion dispersion was obtained by mixing Nafion 117 (Aldrich, 10% dispersion in water) with an equal volume of 0.10 M HEPES buffer, pH 7, and adjusting the pH of the mixture with a solution of NaOH. A stock dispersion of carbon black particles (XC72R, Cabot Corp., 20 mg mL^{-1}) was prepared by ultrasonication (5 min) in 0.10 M HEPES, pH 7. To prepare the carbon particle network, 2 μL of Nafion dispersion was combined with 1.5 μL of carbon particle suspension and 25 μL of Hyd2 (88 μM) and allowed to dry partially on the ATR prism. Spectroelectrochemistry was carried out using a custom-modified ATR-IR accessory (GladiATR, PIKE Technologies) and a Varian 680-IR spectrometer. Data collection and analysis were performed using Varian Resolutions Pro 4.0 software. Spectra were recorded at 4 cm^{-1} resolution and are reported as an average of 500 scans as difference spectra (final potential minus starting potential) following subtraction of a linear baseline. Electrochemical control was provided by an Autolab PGSTAT 128N potentiostat manipulated by Nova software (EcoChemie). Potentials are quoted with respect to SHE using the correction $E_{SHE} = E_{SCE} + 242$ mV at 25 °C.

Prior to spectroscopic experiments, as-isolated Hyd2 was activated at −600 mV vs SHE with H_2-saturated buffer (0.10 M HEPES, pH 7, 0.10 M NaCl) pumped through the spectroelectrochemical cell for 3 h. The H_2 was then removed from the cell solution by bubbling with N_2. The potential was then stepped to a starting value to record a background spectrum, and difference spectra were collected at 100 mV potential intervals as the potential was stepped to more positive values, with data collection at 20 min after each potential step. The experiment was repeated with 10 mM cyanide (final concentration) introduced into the cell solution at low potential before commencing the potential steps as described above.

RESULTS

Figure 2A shows the effect of cyanide on the activity of the O_2-sensitive *Escherichia coli* [NiFe]-hydrogenase-2 over a potential range of 810 mV. The potential was cycled between −520 and +290 mV at 4 mV s^{-1}. Two cycles were completed in the absence of cyanide (shown in red) before an aliquot of KCN solution was injected into the electrochemical cell at the start of the oxidative sweep, leading to a concentration of 1.40 mM KCN in the cell immediately following the injection at the start of scan 3.

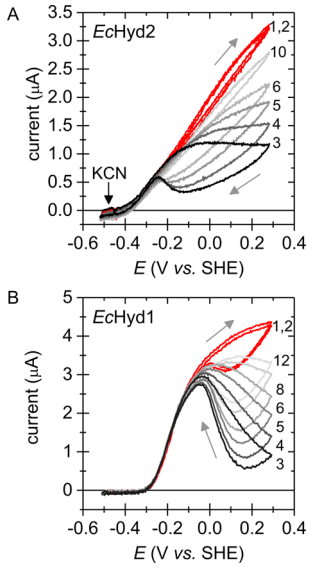

Figure 2. Effect of cyanide on Hyd2 (A) and Hyd1 (B) when introduced at −520 mV during a set of cyclic voltammetry scans (scan number is indicated alongside each plot). To minimize the rate at which HCN was flushed out of the cell, the electrode was rotated at 100 rpm and there was no gas flow through the cell. Scans prior to the introduction of cyanide are shown in red, and those after are shown in shades of gray. Other conditions: pH 7; 25 °C; scan rate = 4 mV s^{-1}. The final concentration of KCN in the cell immediately after the injection was 1.4 mM. The buffer was equilibrated with 100% H_2, 1 atm) before the start of each experiment. Gray arrows indicate the direction of the scan.

Introducing cyanide has no effect on the H^+ reduction or H_2 oxidation activity below approximately −250 mV, but as the potential is swept to more positive values, the presence of cyanide results in a marked decrease in current compared to when no cyanide is present. The inactivation that is demonstrated by the drop in current continues throughout the cyclic voltammogram until a certain potential is reached upon the return scan (approximately −120 mV) at which point reactivation of the enzyme commences, as seen by a sharp increase in current until, eventually, the activity of the enzyme returns to its uninhibited value.

The inhibitory effect of cyanide is not specific to Hyd2, and corresponding data for an analogous experiment on the O_2-tolerant [NiFe]-hydrogenase-1 (Hyd1) are shown in Figure 2B. In this case, a higher potential is required for cyanide to have an effect, with a decrease in current observed at potentials over −100 mV. Like Hyd2, the inactivation is easily reversed and reactivation occurs during the reductive potential sweep, commencing at potentials below approximately +160 mV. Because of the importance of EPR spectroscopy in interpreting the results, we focused subsequent investigations on Hyd2 rather than Hyd1 because EPR spectra of the latter are complicated by spin coupling to the paramagnetic super-oxidized proximal [4Fe-3S] cluster.[30]

In both panels A and B of Figure 2, successive cycles show a diminishing effect because cyanide is removed from the cell as gaseous HCN. The pK_a for HCN is 9.21,[31] thus essentially all the cyanide in the cell at pH 7 will be in the volatile HCN form. The rate of removal of HCN could be minimized by stopping the gas flow for the duration of the experiment and employing a slow rotation rate (100 rpm) although not so low that H_2 oxidation becomes mass-transport-limited. The Michaelis constants, $K_M^{H_2}$, for Hyd1 and Hyd2 have been calculated to be 9 ± 1 and 17 ± 4 μM, respectively, at −175 mV,[25] values sufficiently low that partial depletion is not an issue given that the experiments were carried out in buffer previously saturated with 1 atm H_2. A comparative experiment for Hyd2 in which gas is flowing through the cell and the electrode rotation rate is set at 3500 rpm, is shown in Supporting Information, Figure S1. Data from UV−visible spectroscopic studies, monitoring the rate at which HCN is removed from the cell, are shown in Figure S2.

In a chronoamperometry experiment, the potential is held at a constant value, allowing current to be measured as a function of time: this deconvolutes the potential and time domain, allowing rates of inactivation/reactivation to be determined. Figure 3A shows experiments in which the potential was held at +394 mV for approximately 200 s before an aliquot of cyanide solution was injected into the cell resulting in final concentrations of 0.05, 0.70, and 1.40 mM cyanide. The rate at which HCN was flushed from the cell was minimized by turning off the gas flow through the cell and using a slow rotation rate. The introduction of cyanide initiates a decrease in the activity of Hyd2 in all cases, with the rate of the inactivation increasing with cyanide concentration. At least 80% of the decrease in current could be fitted to a single exponential

dx.doi.org/10.1021/ja504942h | J. Am. Chem. Soc. 2014, 136, 10470−10477

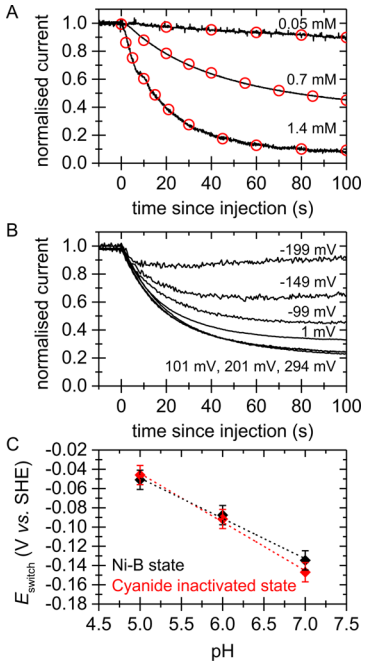

Figure 3. (A) Effect of cyanide on Hyd2 when introduced at +394 mV during a chronoamperometry experiment. An aliquot of cyanide was injected into the cell at t = 0, resulting in final concentrations of 0.05, 0.7, and 1.4 mM. The headspace of the cell and the buffer within it were equilibrated to 100% H_2 prior to the start of each experiment. There was no gas flow though the headspace of the cell during the experiments, and the electrode rotation rate (ω) = 100 rpm. In each case, the first "fast" part of the inactivation, accounting for at least the first three half-lives, has been fitted to a single exponential (red circles). (B) Effect of cyanide (1.4 mM) on Hyd2 when introduced at different potentials, as indicated in the panel. (C) Variation in E_{switch} with pH for the cyanide-inactivated state (red diamonds) and the Ni–B state (black diamonds) for Hyd2. Error bars indicate the experimental error. The line of best fit for each set of data is shown as a dashed line. Conditions unless otherwise specified: 25 °C; pH 7; ω = 3500 rpm; 100% H_2 at 500 sccm; ν = 1 mV s^{-1}. Chronoamperometry data were normalized to account for film loss.

(shown as circles), showing that the reaction is first-order in active Hyd2, but as explained later, more extensive studies made use of initial rate analysis. Figure 3B shows the influence of electrode potential upon the rate and extent of inactivation. The initial rate of inactivation upon injection of KCN solution is similar in all cases, whereas the extent of inactivation first increases then levels off above +100 mV.

Further electrochemistry experiments were carried out to investigate the nature of the reactivation observed at low potentials in Figure 2A. The parameter "E_{switch}" has previously been used to compare different potential-dependent inactive states and the ease with which they can be reactivated in various hydrogenases.[25] Typically, E_{switch} is estimated from the first derivative of the reductive sweep directly following complete inactivation and is defined as the local minimum in the high-potential region.[26] To measure E_{switch}, the enzyme was first oxidatively inactivated and then reductively reactivated to the maximum extent in both cases. To achieve this aim, a potential of +394 mV was applied while KCN solution was injected into the cell solution which had previously been equilibrated with an atmosphere of 10% H_2 in Ar. For this part of the experiment, the gas flow was turned off and a slow rotation rate was used in order to minimize the rate at which HCN was flushed from the cell. These conditions were maintained for approximately 1000 s, ensuring a limiting current had been reached, before the gas flow was turned back on at 100% H_2 (500 sccm) and the rotation rate set to 3500 rpm. To ensure full equilibration of the cell solution and full removal of cyanide, these conditions were maintained for 800 s before a cyclic voltammetry scan was started from high to low potential at a scan rate of 1 mV s^{-1}. The E_{switch} value obtained for the cyanide-inactivated state was compared to that of the well-characterized Ni–B state made anaerobically by applying a potential of +394 mV to the enzyme film under 100% Ar. After the enzyme had fully inactivated (approximately 4000 s), the cell was re-equilibrated with 100% H_2 for 1000 s and a cyclic voltammogram was started from high potential at 1 mV s^{-1} as before. These experiments were repeated for pH 5.0, 6.0, and 7.0, and the results are shown in Figure 3C. No significant difference is observed between the E_{switch} values obtained from Hyd2 inactivated via the two different procedures. In both cases, E_{switch} decreases with increasing pH.

A series of experiments was conducted to examine the effects of pH, KCN concentration, and H_2 concentration on rates of oxidative inactivation of Hyd2. First it was established that the rates are independent of pH over the range of 6–8, and data are shown in Supporting Information, Figure S3. To determine an initial rate, that is, the rate obtained within the first few seconds of the reaction before complications such as HCN flushing from the cell become significant, a line of best fit was fitted to the very first part of the inactivation found from experiments similar to those exemplified in Figure 3B. Experiments were carried out at 807 mV above $E(2H^+/H_2)$ under 5, 25, 50, and 100% H_2, with the total gas flow rate set to 500 sccm. In each case, the rate was obtained from the gradient of a slope fitted over the initial linear decrease in current, which ranged from the first 1.5 to 5 s of data, depending upon the KCN concentration used. Figure 4 shows that the rate of inactivation increases with cyanide concentration from 0.05 to 1.4 mM then levels off. The solid lines are fits to a global analysis that will be explained later.

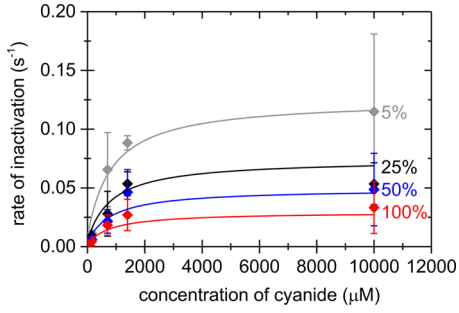

Figure 4. Relationship between the initial rate of inactivation of Hyd2 and the concentration of cyanide injected into the cell under different H_2 atmospheres as indicated in the figure. An aliquot of cyanide was injected into the cell during a chronoamperometry experiment at 807 mV above $E(2H^+/H_2)$ resulting in final concentrations of 0.05, 0.15, 0.70, 1.40, and 10 mM. Other conditions: pH 7, 25 °C, electrode rotation rate = 3500 rpm, total gas flow = 500 sccm. In each case, the rate was obtained from a linear fit to the initial part of the inactivation current. Lines show a global fit of eq 1 to the data (see Discussion). The value of k_1 was estimated to be 0.01 s^{-1}. Using this value, the values of the other parameters obtained from the fit are as follows: $K_d^{H_2}$ = 0.24 bar, K_d^{CN} = 0.84 mM, and k_2 = 0.14 s^{-1}.

dx.doi.org/10.1021/ja504942h | J. Am. Chem. Soc. 2014, 136, 10470–10477

Spectroscopic experiments were now carried out to establish whether new species could be detected in the presence of cyanide, under oxidizing conditions. Importantly, these experiments were carried in the absence of H_2, in contrast to the PFE experiments where H_2 is essential in order to observe the reaction.

Electron paramagnetic resonance was used to test for the appearance of any new species with unpaired electrons formed during the reaction of Hyd2 (see Materials and Methods) with KCN under oxidizing conditions. Two samples, equilibrated at +413 and +416 mV, respectively, are compared in Figure 5.

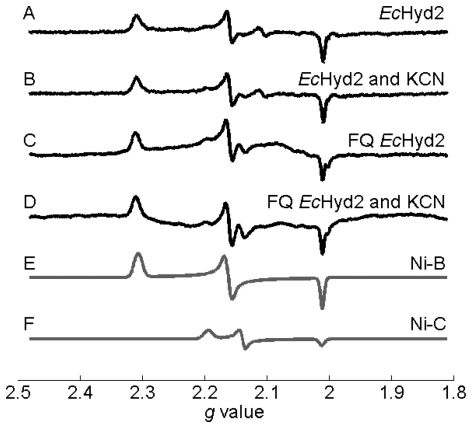

Figure 5. X-band continuous wave EPR spectra of Hyd2 oxidized in the presence and absence of cyanide. The exact conditions of each sample are as follows: (A) Hyd2 and $K_3[Fe(CN)_6]$ only, potential = +413 mV; (B) Hyd2, KCN (5 mM), and $K_3[Fe(CN)_6]$, potential = +416 mV; (C) Hyd2 and $K_3[Fe(CN)_6]$ (4.8 mM) only; (D) Hyd2, KCN (5.1 mM), and $K_3[Fe(CN)_6]$ (4.8 mM); (E) simulation of the Ni–B state; and (F) simulation of the Ni–C state. Spectra (C) and (D) were obtained using a freeze-quench (FQ) method with 4 mm high precision tubes. Other conditions: pH 7; temperature, 80 K; microwave power, 2 mW; microwave frequency, 9.381 GHz (spectra A and B) and 9.375 GHz (spectra C and D); 100 kHz; field modulation amplitude, 0.5 mT (spectra A and B) and 1 mT (spectra C and D).

Sample A contains only Hyd2 and the oxidant $K_3[Fe(CN)_6]$, whereas sample B also contains 5.1 mM KCN. Sample A shows a clear rhombic signal with g values of g_x = 2.31, g_y = 2.16, and g_z = 2.01, unambiguously attributable to the Ni–B (Ni(III)) state of Hyd2.[25] Another faint signal is observed with g values of g_x = 2.24, g_y = 2.10, and g_z = 2.05, similar to that observed for the regulatory [NiFe]-hydrogenase of *Ralstonia eutropha*.[32] Sample B, which contains KCN, also shows the same EPR spectrum attributed to the Ni–B state as well as the species with g_x = 2.24. No previously unreported signals, or those attributable to Ni–A, can be seen in either spectrum.

In an attempt to observe any new intermediates formed within a second during the reaction of KCN with Hyd2, samples were acquired using a freeze-quench (FQ) technique. Figure 5C,D shows the EPR spectra of samples prepared in this way in which the reaction, initiated by mixing Hyd2 with $[Fe(CN)_6]^{3-}$ either alone or with KCN, was quenched within about 1 s. The important observation is that no previously uncharacterized species appears on this time scale. The procedure is not reliable enough to provide kinetic information: samples C and D both show signals attributable to Ni–B, which was difficult to avoid in the starting material (prepared by removing H_2 without potential control), and faint signals consistent with the active Ni–C state (g_x = 2.19, g_y = 2.14, and g_z = 2.01) are observable in both spectra, to a greater degree than observed with the equilibrated samples.

To check for the presence of new species regardless of redox and spin state, experiments were carried out using ATR-IR spectroelectrochemistry. This technique[29] allows unmediated electrochemical control of the enzyme, which is contained within a gastight ATR-IR cell and simultaneous collection of infrared spectra. Use of an all-carbon working electrode instead of a noble metal avoids the possibility of the electrode reacting with solutes such as KCN which can be introduced to the cell during an experiment. Figure 6 shows redox-triggered difference spectra (background recorded at −400 mV) recorded under N_2 as the potential was stepped to more positive values in 100 mV intervals up to 0 mV, with and without KCN present. The spectra presented were recorded 20 min after each potential step, at which point the enzyme was found to have reached diffusion-controlled equilibrium with the electrode potential. Only the changes in absorbance attributed to the endogenous CO ligand, ν(CO), are well resolved (1900–2000 cm^{-1} region). The greater intensity of the ν(CO) peaks compared to those resulting from vibrations of the endogenous CN^- ligands, ν(CN), 2050–2150 cm^{-1} region, mean that ν(CO) features are of greater benefit in identifying states and characterizing new species.

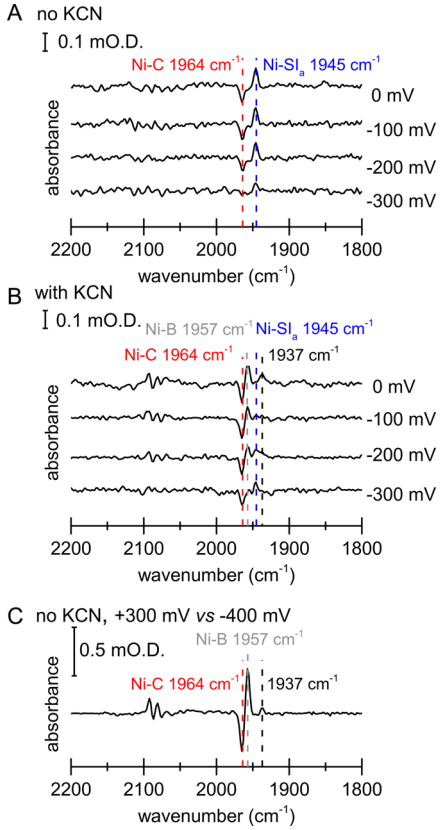

Figure 6. ATR-IR redox-triggered difference spectra of Hyd2 at a carbon particle electrode. (A,B) Background spectra were collected at −400 mV, followed by potential steps in 100 mV intervals. Each spectrum was recorded 20 min after the potential step: (A) without cyanide present; (B) 10 mM KCN present; (C) redox-triggered difference spectrum (+300 mV minus −400 mV) of Hyd2 with no cyanide present. All spectra were recorded in N_2-saturated buffer (0.10 M HEPES, pH 7, containing 0.10 M NaCl).

dx.doi.org/10.1021/ja504942h | J. Am. Chem. Soc. 2014, 136, 10470–10477

Scheme 2. Mechanism by Which Cyanide Facilitates the Formation of Ni−B Showing Plausible Cyanide Intermediates[a]

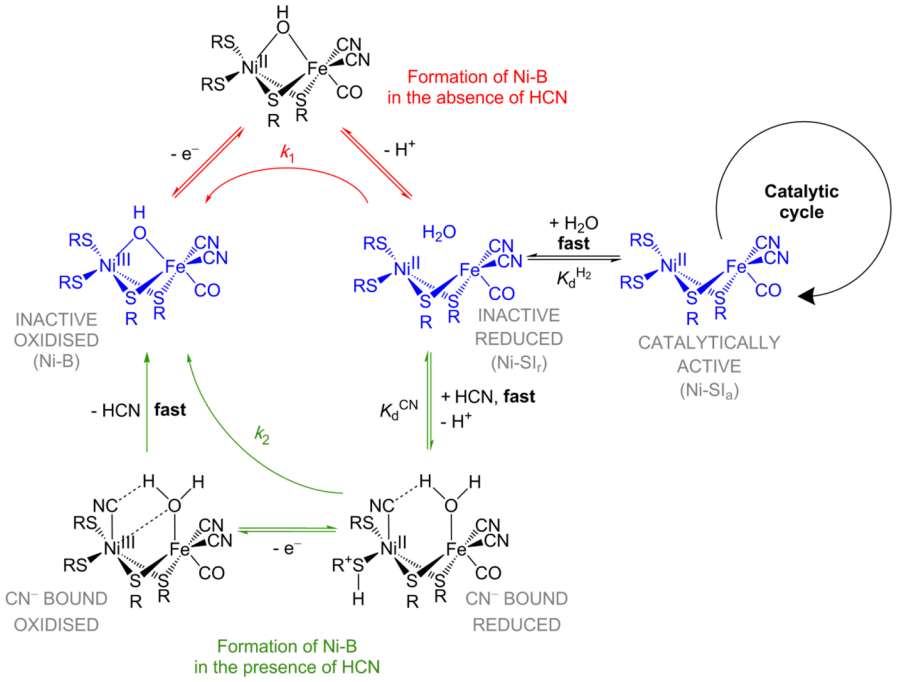

[a]Well-characterized states are shown in blue. Red arrows indicate a pathway leading to the formation of the Ni−B state under normal conditions (in the absence of cyanide), whereas green arrows indicate a possible pathway for Ni−B formation which may occur in the presence of cyanide.

As shown in the difference spectra in Figure 6A, steps from −400 mV to 0 mV resulted in the appearance of a negative band at 1964 cm^{-1}, consistent with loss of the Ni−C state, and growth of a band at 1945 cm^{-1}, consistent with formation of the Ni−SI_a state (also known as Ni−S). The band positions for these states correspond most closely to the ν(CO) features observed for the [NiFe]-hydrogenase of *Desulfovibrio vulgaris* as studied by Fichtner et al.[33]

Figure 6B depicts an analogous set of redox-triggered difference spectra recorded after introducing 10 mM KCN (final concentration) into the cell solution in contact with the enzyme sample. In the presence of cyanide, a growth band at 1957 cm^{-1} is now obvious at −200 mV, accompanied by a weaker band at 1945 cm^{-1}. As the potential is stepped to −100 mV and then 0 mV, the band at 1957 cm^{-1} continues to grow, and the 1945 cm^{-1} band disappears. The 1957 cm^{-1} peak corresponds well with ν(CO) reported for the Ni−B state in the *D. vulgaris* hydrogenase (1955 cm^{-1}). This assignment is confirmed by examination of the difference spectrum in Figure 6C, recorded in the absence of cyanide after holding the potential at +300 mV for 20 min, which also shows growth of an intense positive band at 1957 cm^{-1}. A weak feature is visible at 1937 cm^{-1} in the spectra of both Figure 6B,C and may correspond to a small portion of the Ni−SI_r state. Thus, the spectra recorded in the presence of cyanide indicate almost complete conversion of Ni−C to Ni−B after 20 min at 0 mV, whereas in the analogous experiment conducted in the absence of cyanide (Figure 6A), Ni−C converts only to Ni−SI_a under the same conditions. No additional ν(CO) peaks can be identified in the spectra for Hyd2 in the presence of cyanide, showing that no intermediate in the cyanide reaction is observed.

DISCUSSION

These results demonstrate an important reaction between cyanide and [NiFe]-hydrogenases that is revealed in clear detail by protein film electrochemistry and investigated further by spectroscopy. As observed in Figures 2 and 3, the introduction of cyanide accelerates the high potential inactivation that occurs in Hyd1 and Hyd2 but has no effect on the activity of either enzyme at low potentials. The potential dependence is consistent with cyanide targeting the active site of the enzyme—not a species that is directly in the catalytic cycle (such an interaction would result in a decrease in H_2 oxidation current regardless of electrode potential) but a species that is in rapid equilibrium with active states and can be removed by oxidation as the potential is increased. For both Hyd1 and Hyd2, cyclic voltammograms show that this inactivation is reversed simply by applying a reducing potential.

Chronoamperometry experiments show that a limiting current is established after the initial inactivation caused by cyanide (Figure 3A,B), indicating that an equilibrium is set up between active enzyme and the cyanide-inactivated state. Three experiments, investigating the effect of cyanide over nearly a 200 mV window from +101 to +294 mV, show almost identical inactivation characteristics (Figure 3B) consistent with the rate of inactivation being unaffected by potential in this region. Below approximately 0 mV, the extent of reaction decreases as reactivation becomes increasing favorable.

Any reasonable mechanistic proposal must account for the observations that the rate of inactivation increases to a limiting value as the cyanide concentration is raised and decreases as $[H_2]$ is increased. There is no evidence for a previously uncharacterized state, although one might be observed at reaction times shorter than we were able to achieve. The characteristic reactivation potentials E_{switch} coincide closely with those observed for the Ready state (Ni−B) formed simply

dx.doi.org/10.1021/ja504942h | J. Am. Chem. Soc. 2014, 136, 10470−10477

upon anaerobic oxidation, albeit much more slowly; likewise, the EPR and ATR-IR spectra of the product formed between Hyd2 and cyanide whether at equilibrium or quenched within approximately 1 s reveal only the formation of Ni−SI_a and Ni−B states (Figures 5 and 6). The lack of detection of any intermediate species in samples obtained within approximately 1 s (Figure 5, samples C and D) suggests three possibilities: (i) a key intermediate species is not EPR-active; (ii) the reaction was not quenched on a sufficiently fast time scale; and (iii) the concentration of the intermediate at any time is not high enough to be detected by EPR. When Hyd2 is exposed to the oxidant $[Fe(CN)_6]^{3-}$, the well-characterized Ni−B state is the final product, regardless of whether cyanide is assisting the reaction. The ATR-IR spectroelectrochemical experiments (Figure 6) show that in the presence of cyanide more Ni−SI_a has converted to Ni−B after 20 min.

These results lead us to conclude that cyanide acts as a strong promoter of Ni−B formation. The mechanism outlined in Scheme 2 forms the basis of the rate law 1, which is derived in approximate form in Supporting Information. The intermediates are plausible: we require that CN^- binds to the Ni and a weakly bound water molecule is also in place (we have placed it on the Fe). To simplify the derivation, it was assumed that the rates are independent of pH (as observed between pH 6 and 8) and electrode potential (which is true above a potential of +100 mV; see Figure 3B). The free cyanide species in solution is assumed to be HCN (as also confirmed by ATR-IR under the same conditions). In eq 1 (see Supporting Information)

$$k_{obs} = \frac{k_1 K_d^{H_2}}{(K_d^{H_2} + [H_2])} + \frac{k_2 K_d^{H_2}[HCN]}{(K_d^{CN} + [HCN])(K_d^{H_2} + [H_2])} \quad (1)$$

k_{obs} is the rate constant for inactivation as observed in electrochemistry experiments, k_1 is the rate constant for formation of Ni−B in the absence of cyanide, k_2 is the rate constant for the cyanide-dependent pathway, and $K_d^{H_2}$ and K_d^{CN} are dissociation constants for H_2 and cyanide, respectively, leading back to the first inactive state (depicted in Scheme 2 as Ni−SI_r). Figure 4 shows a global fit, with values of $K_d^{H_2}$, K_d^{CN}, and k_2 held constant over the data obtained from all H_2 concentrations studied. Equation 1, although derived using a simplified version of the mechanism proposed in Scheme 2, gives a good overall fit to the data and is instructive. According to the analysis, cyanide gives at least a 14-fold increase in the rate of Ni−B formation (0.14/0.01). The value $K_d^{H_2}$ = 0.24 bar reflects the relatively low affinity of H_2 for the Ni−SI_r state (binding is much weaker than is normally reflected in K_M values that represent the interaction of H_2 with active states) and the value K_d^{CN} = 0.84 mM is also consistent with weak (but fast) binding of cyanide.

Although the exact nature of the normal mechanism leading to formation of Ni−B (i.e., where no cyanide is present) still remains unclear, in electrochemical terms, it is a "CE" reaction; that is, the first step is a chemical reaction, and the second step is an electron transfer.[26] Under anaerobic conditions, the chemical process is likely to entail the transport of a H_2O molecule into the active site (converting Ni−SI_a into Ni−SI_r) and eventual coordination of a OH^- ligand to the Ni. This chemical step is then followed by a rapid electron transfer in which Ni(II) is oxidized to Ni(III), thus trapping the OH^- as a bridging ligand. Cyanide is clearly a potent inactivator, but unlike CO, it does not affect H_2 oxidation unless a more oxidizing potential is applied: this requires the participation of at least two more intermediates. One is formed as a result of CN^- binding rapidly to the active site in the inactive reduced state Ni−SI_r (most likely after entering the site as HCN) producing a weakly bound Ni(II)−CN species. Cyanide is a better nucleophile than OH^- (and much better than H_2O),[34,35] and there are numerous examples of Ni(II)−CN complexes in the literature.[36,37] With the additional strong σ-donor CN^- now in place, albeit weakly bound, the Ni(II) is poised for oxidation to Ni(III), and the second species, a short-lived Ni(III)−CN complex, is formed upon electron transfer. Studies of Ni(III)−cyanido complexes have shown that the Ni^{III}−CN bond is labile,[38,39] and a further factor dictates the final course of events, which is that when two metal ions lie in close proximity, OH^- is a very much better *bridging* ligand than CN^-. To our knowledge, there is no evidence of a cyanide ligand bridging two metal ions in a μ_2-C,C conformation[37,40,41] (although there are some instances in which cyanide bridges in a μ_3-C,C,N fashion).[41] Examples of cyanido ligands forming linear bridges (μ_2-C,N) are well-known,[36,37,42] but the small 2.6 Å space[43] between the metal atoms in the active site makes a μ_2-C,N bridge an unlikely possibility. Conversely, hydroxide is an excellent μ_2-O,O bridging ligand across 2.6 Å, and numerous examples of a hydroxide ligand acting in this way can be found.[40]

In summary, the large rate enhancement for oxidative formation of the oxidized "resting" Ni−B state in the presence of cyanide can be attributed to a terminal CN species being the *kinetically* preferred product (compared to a terminal Ni(III)−OH species). Cyanide is a much better nucleophile than OH^- and therefore facilitates the oxidation of Ni(II) to Ni(III) which depends upon an additional donor ligand being coordinated. However, the greater stability afforded when CN^- is subsequently replaced by OH^-, which can form a stable bridge between Ni(III) and Fe(II), results in rapid conversion to Ni−B which is the *thermodynamic* product. An analogous observation is made for Hyd1, indicating that the accelerated formation of the Ni−B state in the presence of cyanide is not specific to Hyd2. We can now comment upon observations first made during the infancy of biohydrogen research that could not be explained at the time. On the one hand, it is now clear why cyanide was only an inhibitor under oxidizing conditions;[7,8] on the other hand, our results show clearly that the inhibition caused by cyanide is simply reversed upon reduction, and cyanide does not remain bound at the active site once it has performed its role in facilitating formation of the oxidized resting state. The experiments serve as a further example of how protein film electrochemistry, with its special capability for examining the catalytic activity of a minuscule, immobilized enzyme sample as a detailed function of potential as well as time, helps to resolve a puzzle that has remained a mystery throughout the history of hydrogenase research.

■ ASSOCIATED CONTENT

Supporting Information

Effect of cyanide when introduced at a low potential. Measuring the time course of HCN evaporation from the cell. Effect of pH on the rate of inactivation of Hyd2 by cyanide. The basis of eq 1. This material is available free of charge via the Internet at http://pubs.acs.org.

AUTHOR INFORMATION

Corresponding Authors

fraser.armstrong@chem.ox.ac.uk
kylie.vincent@chem.ox.ac.uk

Notes

The authors declare no competing financial interest.

ACKNOWLEDGMENTS

This research was supported by the Biological and Biotechnological Sciences Research Council (Grants BB/H003878-1, BB/I022309-1, and BB/L009722/1 to F.A.A.), the Engineering and Physical Sciences Research Council (Supergen V Grant EP/H019480/1 to F.A.A.), and the European Research Council (Grant EnergyBioCatalysis-ERC-2010-StG-258600ERC to K.A.V.). M.W.C. is grateful for the support of a University of Oxford Clarendon Fund Scholarship. We thank Elena Nomerotskaia for preparing samples of Hyd1 and Hyd2. F.A.A. is a Royal Society-Wolfson Research Merit Award holder.

REFERENCES

(1) Vincent, K. A.; Cracknell, J. A.; Lenz, O.; Zebger, I.; Friedrich, B. R.; Armstrong, F. A. *Proc. Natl. Acad. Sci. U.S.A.* **2005**, *102*, 16951.
(2) Pandelia, M. E.; Ogata, H.; Currell, L. J.; Flores, M.; Lubitz, W. *Biochim. Biophys. Acta, Bioenerg.* **2010**, *1797*, 304.
(3) Pandelia, M. E.; Infossi, P.; Giudici-Orticoni, M. T.; Lubitz, W. *Biochemistry* **2010**, *49*, 8873.
(4) Léger, C.; Dementin, S.; Bertrand, P.; Rousset, M.; Guigliarelli, B. *J. Am. Chem. Soc.* **2004**, *126*, 12162.
(5) Goldet, G.; Brandmayr, C.; Stripp, S.; Happe, T.; Cavazza, C.; Fontecilla-Camps, J. C.; Armstrong, F. A. *J. Am. Chem. Soc.* **2009**, *131*, 14979.
(6) Lee, S. B.; Wilson, J. B.; Wilson, P. W. *J. Biol. Chem.* **1942**, *144*, 273.
(7) Hyndman, L. A.; Burris, R. H.; Wilson, P. W. *J. Bacteriol.* **1953**, *65*, 522.
(8) Seefeldt, L. C.; Arp, D. J. *J. Bacteriol.* **1989**, *171*, 3298.
(9) Volbeda, A.; Montet, Y.; Vernède, X.; Hatchikian, E. C.; Fontecilla-Camps, J. C. *Int. J. Hydrogen Energy* **2002**, *27*, 1449.
(10) Volbeda, A.; Garcin, E.; Piras, C.; de Lacey, A. L.; Fernandez, V. M.; Hatchikian, E. C.; Frey, M.; Fontecilla-Camps, J. C. *J. Am. Chem. Soc.* **1996**, *118*, 12989.
(11) Pandelia, M. E.; Ogata, H.; Lubitz, W. *ChemPhysChem* **2010**, *11*, 1127.
(12) Montet, Y.; Amara, P.; Volbeda, A.; Vernede, X.; Hatchikian, E. C.; Field, M. J.; Frey, M.; Fontecilla-Camps, J. C. *Nat. Struct. Biol.* **1997**, *4*, 523.
(13) Teixeira, V. H.; Baptista, A. M.; Soares, C. M. *Biophys. J.* **2006**, *91*, 2035.
(14) Ogata, H.; Mizoguchi, Y.; Mizuno, N.; Miki, K.; Adachi, S.; Yasuoka, N.; Yagi, T.; Yamauchi, O.; Hirota, S.; Higuchi, Y. *J. Am. Chem. Soc.* **2002**, *124*, 11628.
(15) Lubitz, W.; Reijerse, E.; van Gastel, M. *Chem. Rev.* **2007**, *107*, 4331.
(16) Siegbahn, P. E. M.; Tye, J. W.; Hall, M. B. *Chem. Rev.* **2007**, *107*, 4414.
(17) Volbeda, A.; Martin, L.; Cavazza, C.; Matho, M.; Faber, B. W.; Roseboom, W.; Albracht, S. P. J.; Garcin, E.; Rousset, M.; Fontecilla-Camps, J. C. *J. Biol. Inorg. Chem.* **2005**, *10*, 239.
(18) Gastel, M.; Stein, M.; Brecht, M.; Schroeder, O.; Lendzian, F.; Bittl, R.; Ogata, H.; Higuchi, Y.; Lubitz, W. *J. Biol. Inorg. Chem.* **2006**, *11*, 41.
(19) Cracknell, J. A.; Wait, A. F.; Lenz, O.; Friedrich, B.; Armstrong, F. A. *Proc. Natl. Acad. Sci. U.S.A.* **2009**, *106*, 20681.
(20) Vincent, K. A.; Parkin, A.; Lenz, O.; Albracht, S. P. J.; Fontecilla-Camps, J. C.; Cammack, R.; Friedrich, B.; Armstrong, F. A. *J. Am. Chem. Soc.* **2005**, *127*, 18179.
(21) Vincent, K. A.; Belsey, N. A.; Lubitz, W.; Armstrong, F. A. *J. Am. Chem. Soc.* **2006**, *128*, 7448.
(22) Higuchi, Y.; Ogata, H.; Miki, K.; Yasuoka, N.; Yagi, T. *Struct. Fold. Des.* **1999**, *7*, 549.
(23) Léger, C.; Elliott, S. J.; Hoke, K. R.; Jeuken, L. J. C.; Jones, A. K.; Armstrong, F. A. *Biochemistry* **2003**, *42*, 8653.
(24) Vincent, K. A.; Parkin, A.; Armstrong, F. A. *Chem. Rev.* **2007**, *107*, 4366.
(25) Lukey, M. J.; Parkin, A.; Roessler, M. M.; Murphy, B. J.; Harmer, J.; Palmer, T.; Sargent, F.; Armstrong, F. A. *J. Biol. Chem.* **2010**, *285*, 3928.
(26) Jones, A. K.; Lamle, S. E.; Pershad, H. R.; Vincent, K. A.; Albracht, S. P. J.; Armstrong, F. A. *J. Am. Chem. Soc.* **2003**, *125*, 8505.
(27) Stoll, S.; Schweiger, A. *J. Magn. Reson.* **2006**, *178*, 42.
(28) Dutton, P. L. *Methods Enzymol.* **1978**, *54*, 411.
(29) Healy, A. J.; Ash, P. A.; Lenz, O.; Vincent, K. A. *Phys. Chem. Chem. Phys.* **2013**, *15*, 7055.
(30) Roessler, M. M.; Evans, R. M.; Davies, R. A.; Harmer, J.; Armstrong, F. A. *J. Am. Chem. Soc.* **2012**, *134*, 15581.
(31) Ang, K. P. *J. Chem. Soc.* **1959**, 3822.
(32) Bernhard, M.; Buhrke, T.; Bleijlevens, B.; de Lacey, A. L.; Fernandez, V. M.; Albracht, S. P. J.; Friedrich, B. *J. Biol. Chem.* **2001**, *276*, 15592.
(33) Fichtner, C.; Laurich, C.; Bothe, E.; Lubitz, W. *Biochemistry* **2006**, *45*, 9706.
(34) Pearson, R. G.; Sobel, H.; Songstad, J. *J. Am. Chem. Soc.* **1968**, *90*, 319.
(35) Swain, C. G.; Scott, C. B. *J. Am. Chem. Soc.* **1953**, *75*, 141.
(36) Greenwood, N. N.; Earnshaw, A. *Chemistry of the Elements*, 2nd ed.; Butterworth-Heinemann: Oxford, UK, 1997.
(37) Griffith, W. P. *Q. Rev., Chem. Soc.* **1962**, *16*, 188.
(38) Murray, C. K.; Margerum, D. W. *Inorg. Chem.* **1982**, *21*, 3501.
(39) Pappenhagen, T. L.; Margerum, D. W. *J. Am. Chem. Soc.* **1985**, *107*, 4576.
(40) Cotton, F. A.; Wilkinson, G.; Bochmann, M.; Murillo, C. *Advanced Inorganic Chemistry*, 6th ed.; Wiley: New York, 1998.
(41) Pike, R. D. *Organometallics* **2012**, *31*, 7647.
(42) Gardner, M. T.; Deinum, G.; Kim, Y.; Babcock, G. T.; Scott, M. J.; Holm, R. H. *Inorg. Chem.* **1996**, *35*, 6878.
(43) Ogata, H.; Hirota, S.; Nakahara, A.; Komori, H.; Shibata, N.; Kato, T.; Kano, K.; Higuchi, Y. *Structure* **2005**, *13*, 1635.